Journal of Bio- and Tribo-Corrosion (2023) 9:56
https://doi.org/10.1007/s40735-023-00755-8

Tribo Mechanical Study on Aluminium A356 Reinforced Metal Matrix Composites Casted with Copper Chill

M. Sunil Kumar[1] · N. Sathisha[2] · N. Jagannatha[3]

Received: 2 February 2023 / Revised: 6 March 2023 / Accepted: 24 March 2023 / Published online: 23 June 2023

Abstract

In this research, an effort has been made to examine how copper chill affects the mechanical and tribological characteristics of Aluminium Metal Matrix Composites (AMMCs). The particles of hematite are employed as reinforcement in the A356 alloy's metal matrix at various weight percentage ranges ranging from 0 to 12 wt% in 3 wt% phases. The composite was developed using a sand casting procedure with and without copper chills. Experiments were carried out to evaluate the mechanical and abrasive wear behaviour of composites utilising tensometers and three body abrasive wear testing equipment. The parameters such as both speed and duration were kept constant with changing applied load. Composites casted with copper chills demonstrated superior mechanical and abrasive wear resistance as compared to composites casted without copper chills. Micrographic examination was carried out using X-Ray Diffraction (XRD) patterns and Scanning Electron Microscope (SEM) images. Hematite particles were confirmed to exist by XRD, and it was discovered that they were distributed uniformly throughout the A356 matrix alloy of composites cast with copper chills. The fine-grained structure was obtained as a result of rapid cooling, which had an impact on enhancing mechanical and abrasive wear resistance in composites with copper chills. It was noticed from SEM photos that the fractography images display a brittle mode of fracture. It was also discovered that the worn-out surface of the 9 wt% composites cast with copper chills is smoother than that of the composites cast without copper chills.

Keywords AMMCs · A356 · Hematite · Chill casting · Dry abrasive wear · Microstructure

1 Introduction

Aluminium alloys are now used dynamically in industries to attain improved results. Due to their exceptional toughness, strength, and hardness, as well as their resistance to wear and corrosion. AMMCs are widely used in precincts like automotive, military, and aircraft, amongst others [1–3]. The addition of particles of hematite (particles of hard ceramic iron ore) to aluminium increases its wear and tear characteristics [4]. Superior sand casting must be found by utilising metallic end chills, such as copper, which impacts the microstructure, tribological, and mechanical characteristics [4, 5].

✉ M. Sunil Kumar
suniltiptur404@gmail.com

[1] VTU-RRC, Belgaum, Karnataka, India

[2] Mechanical Engineering, YIT, Mangalore, Karnataka, India

[3] Mechanical Engineering, SJMIT, Chitradurga, Karnataka, India

Chill casting using a sand mould employing liquid metallurgical way, is one of the most effective and extensively utilised methods for MMC castability [6]. Gowda et al. [7], studied the A356 alloy based hybrid composites were invented using stir casting with 1%, 2%, 3%, 4%, and 5% RHA fractions and Al_2O_3 particles in equal extents. Tensile strength and hardness of the mixtures were estimated and the results reveal that the reinforcement addition resulted in a significant improvement in the characteristics. Furthermore, when compared to as cast composite specimens, the heat treated composite specimens shows improved characteristics. Kumar et al. [8], studied the Al AA6063 hybrid metal matrix composite were manufactured through stir casting method with fixed SiC content of 1 wt% and varied TiC content of 1–2.5 wt% in steps of 0.5%. The microstructure, mechanical (hardness) and tribological (pin on disc) properties were estimated and the results depicts that hardness and wear rate increases with increase in reinforcement but density decreases with increase in reinforcement. Jamwal et al. [9], Investigated the mechanical and tribological

properties of Al-1100 reinforced with different weight fractions of Al_2O_3 (2.5, 5, 7.5, 10%) and TiC (2.5, 5, 7.5, 10%) were fabricated through stir casting manner. Mechanical and tribological properties were studied. It was found that addition of reinforced particles with the alumina particles shows maximum tensile strength, hardness, and wear resistance than the unreinforced aluminium. Opapaiboon et al. [10] examine the influence of Cr content on three-body-type abrasive wear conduct of multi-alloyed white cast iron and samples with varied Cr content from 3 to 9 mass% under basic alloy composition were prepared. Three different temperatures were used to temper annealed samples after hardening them between 1323 and 1373 K. The prepared specimens were subject to dry abrasive wear test. Result revels that the value of the wear rate (*R*w) reduced to 6 mass%Cr, and then, increased gradually as Cr content increased. And also As-hardened specimens exhibited higher resistance of wear than tempered specimens. Rakshath et al. [11] studied the dry sliding and abrasive wear behaviour of Al alloy of 7075 reinforced with different weight fractions of alumina and hexagonal boron nitrate filers casted via stir casting method. The prepared specimens were exposed to microstructure, mechanical, dry sliding, sand abrasive wear test. Result shows that both alumina and hexagonal boron nitride fillers shows improved mechanical and wear resistance properties, the reinforced composite specimens shows better resistance against abrasion, than as-cast specimens. Bandekar et al. [12], studied the fractographic and abrasion behaviour (3 body type) of Al LM13 alloy reinforced with various weight fractions of garnet particles of size 25 µm and self-lubricating carbon of particle size 45 µm, hybrid composites were fabricated via sand casting followed through stir casting method. The prepared specimens were subjected to microstructure, mechanical, fractographic, and three body abrasion test. The microstructure results reveals that even dispersal of reinforcements with less clustering. The inclusion of garnet and carbon reinforcement reduces hybrid composites' abrasive wear rate. The fractography behaviour demonstrated the transition from ductile to brittle failure mode. The composites wear resistance is improved by directional chilling with copper chill. Vijay Kumar et al. [13] Examine the three-body abrasive wear of A356 aluminium alloy under T6 heat treatment conditions and compare it to that of the A356 base alloy. The criteria used are speed, applied load on the specimen, and number of revolutions or turns. The prepared specimens were subjected to mechanical properties, three body type of abrasive wear test at T6 heat treatment. Result reveals that abrasion resistance increases for T6 heat treated specimens at different speed, load, and number of revolutions.

According to the preceding/previous literature studies, minimal work on tribological studies on A356-hematite composites has been done. An attempt was made in this work, to study the mechanical and abrasive wear actions on consequence of copper chills for the advancement of A356-hematite reinforced composites utilising three body dry sand abrasive wear testing apparatus. The XRD, EDAX, and micrographs are utilised to study the occurrence of reinforcement and microstructure in the prepared composites. During a wear test, the factors such as applied load are varied whilst maintaining speed and time consistent. The composites that were cast with copper chills had superior mechanical and abrasive wear resistance in comparison to the composites of without copper chills.

Table 1 A356 alloy chemical composition

Composition	Percentage
Si	7.24
Mg	0.43
Fe	0.084
Cu	0.011
Mn	0.019
NI	0.026
Zn	0.004
Others	0.029
Al	92.15

Table 2 Hematite chemical composition

Composition	Percentage
Fe_2O_3	81.13
MnO	0.14
MgO	1.55
TiO_2	0.03
Al_2O_3	0.57
CaO	4.8
SiO_2	4.2
Thrashing of detonation	7.58

2 Materials and Procedures

2.1 Selection of Materials

In this current research, alloy of A356 in ingot form was chosen as a matrix substantial due to its numerous functions in the automotive and aerospace industries. As reinforcement, 80–100 µm-sized particulate hematite was chosen. Both the matrix and the reinforcement materials' chemical compositions are listed in Tables 1 and 2, respectively. The additional characteristics of each material are listed in Tables 3 and 4, respectively.

Table 3 A356 alloy properties

Properties	Units	Values
Density	gm/cc	2.67
Colour	—	Silver
Hardness (Brinell)	—	70–105
Tensile strength ultimate	MPa or N/mm^2	234
Tensile strength yield	MPa or N/mm^2	165
Compressive strength	MPa	650
Elastic modulus	GPa	70–80
Poisson's ratio	Nu	0.33
Melting point	°C	557–613

Table 4 Hematite particles properties

Properties	Units	Values
Particle size	Mm	80–100
Density	gm/cc	5.17
Colour	—	Red
Hardness (Mohr's scale)	Kg/mm^2	5.5–6.5
Tensile strength	MPa or N/mm^2	350
elastic modulus	GPa	211
Poisson's ratio	Nu	0.35

Fig. 1 Electric furnace

2.2 Preparation of Composites

The stir casting process was utilised to create the alloy of A356 reinforced with hematite particulated MMCs, as stated below. Figure 1 depicts the melting of A356 alloy in a (6KW) electric resistance furnace upto 752 °C with a stirring speed of 560 rpm. Hematite particles were warmed at 400 °C before being poured into a furnace containing a molten metal alloy of A356 (at 750 °C). The stirring procedure is sustained for several minutes. Finally, continual stirring is ejaculated, well wetting between matrix and reinforcement. The developed molten metal was poured into a warmed sand mould with and without copper chills as shown in Fig. 2. The casting procedure was repeated for varied compositions of reinforcement with matrix material. (weight ratio of hematite particles with base alloy ranging from 0 to 12% in 3 wt% increments). Figure 3 demonstrates how the casting was done by using copper chilling to make a sand mould that was 170 × 200 × 25 mm in size for various reinforcement combinations [14–16].

2.3 Assessment of Specimens

The test specimens were prepared for hardness and tensile strength using brinell hardness testers and tensometer for with and without copper chill. Figures 4 and 5 shows the photographs of the hardness and tensometer (Tensile) specimens before and after test [17, 18]. The tests were conducted in accord with ASTM E10-95 (BHN) and ASTM-E10-M04 (Tennsometer) standards. The specimens were prepared of size 20 mm diameter and 20 mm length and polished by round samples on different grits of emery paper (BHN). A ball indenter with a diameter of 10 mm (HB500) was used to indent 500 kg of load for 30 s. The different locations were tested to thwart the effects of the indenter resting on the harder particles. By measuring the indentation diameter, the hardness of a material was determined. Tensile test specimens with nominal diameters of 9.5 mm and gauge length of 26 mm were prepared [19–21]. The uniaxial load was gradually applied until the specimen failed, and the resulting strain was measured. The fractured tensile specimens were subjected to fractography studies using SEM. The specimens of A356-hematite Particulate composites with and without copper chill were subjected to a three-body abrasive wear test. The test specimens were prepared in accordance with the ASTM G65-81 test standard of rectangular shape measuring 75 × 25 × 8 mm (Fig. 6). The samples were polished metallographically (3.0 µm) as shown in Fig. 7b. In the current study, dry abrasion apparatus with a 228 mm diameter chloro butyl rubber wheel and a speed range of 1 to 200 rpm was used. By loading the lever attached to the specimen holder, the specimen can be held against the rotating wheel. This load causes the specimen to remain in contact with the rubber wheel. As an abrasive media, silica sand with particle size AFS 50/70 (200 µm) was fed into a hopper. The loaded abrasive medium was permitted to fall down the nozzle between the specimen and the revolving wheel at a constant flow rate of 354 g/min (for all test circumstances) and was collected at the bottom of the tester in the abrasive medium collector. The prepared specimen was examined with sand abrasive wear testing equipment as shown in Fig. 7a. The schematic diagram of sand abrasive wear test as shown in

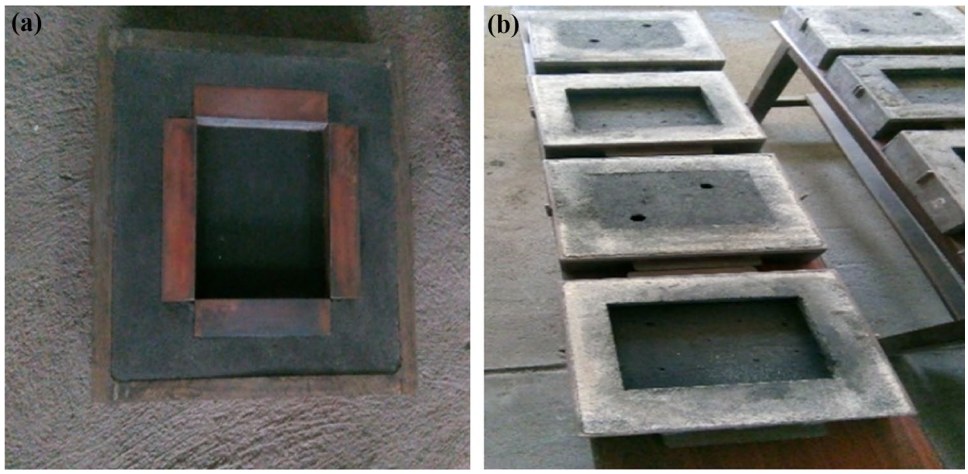

Fig. 2 **a** Mould with Copper chill, **b** Mould without Copper chill

Fig. 3 Prepared Al-A356—hematite composite with Copper chills

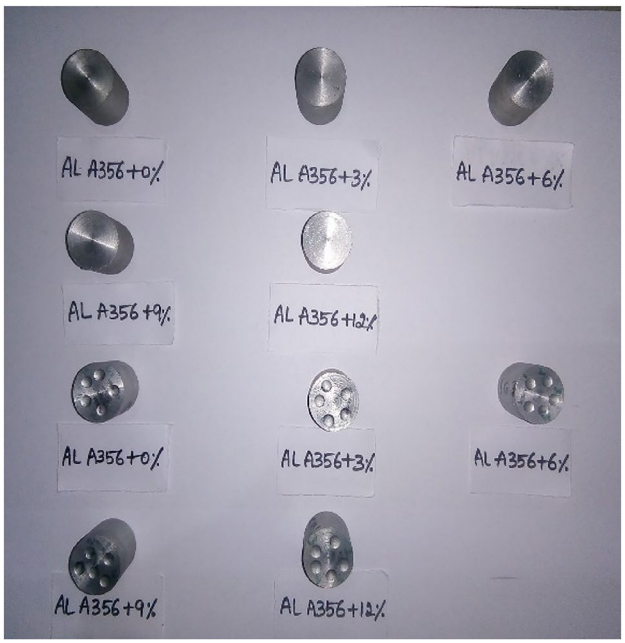

Fig. 4 Brinell Hardness Specimens before and after test

Fig. 6. Tests were carried out for 30 min at 200 rpm (the speed of the rubber wheel) with a load ranging from 2 to 10 KN in steps of 2 KN. Physical wear is caused by the rubbing of sand abrasive particles against the specimen. The variation in the initial and final weights of the specimen before and after test is employed to evaluate wear resistance using weight loss method. The specifications of the tester are reported in Table 5. The abrasion wear rate is given by Eq. (1)

$$W = \Delta G/\rho P \tag{1}$$

where W abrasion wear rate, ΔG weight loss, ρ density of the composite, p applied load

A conventional metallographic procedure was used to prepare the microstructure specimens. The specimen with a diameter of 15 mm and a height of 5 mm was chosen for microstructure investigation. The specimen's surface was grinded (with 240, 600, and 800 µm grind paper) and polished using 44- µm polishing paper. Polishing machine with a velvet cloth was used to attain a smooth surface finish. The samples were washed with distilled water to eliminate impurities such as foreign particles or dust from the surface. Finally, Keller's reagent etched the specimens' surface [22]. Analysing the shape, size, and dispersion of particles of hematite contained in alloy of A356 mixes required the use of a PANA-LYTICAL XRD and CU Kα radiation. The 2θ range was chosen to encompass all of the material phases' intense peaks. The SEM instrument (TESCAN VEGA 3 LMU, Czech Republic) was used to investigate the composites microstructure. For the EDX research connected to the SEM instrument, the JDE 2300 software was utilised [23].

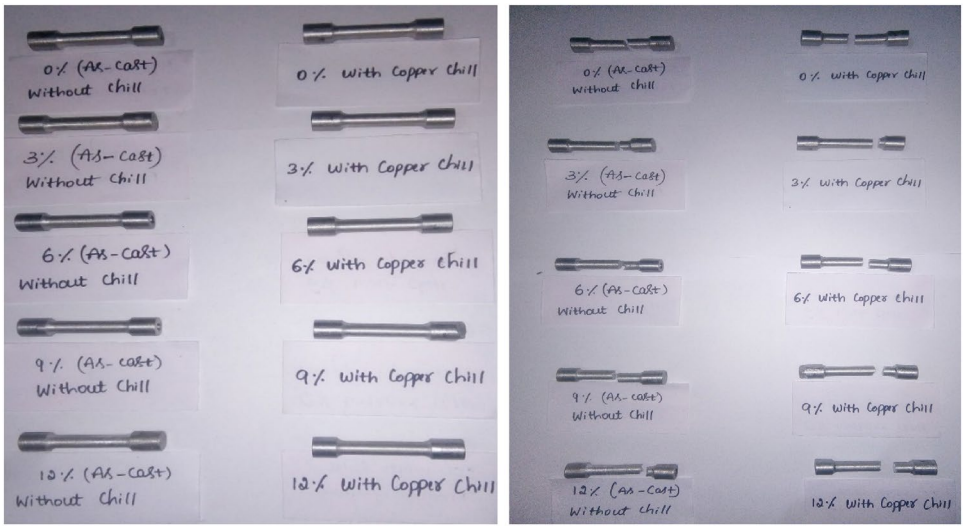

Fig. 5 Tensometer (Tensile) Specimens before and after test

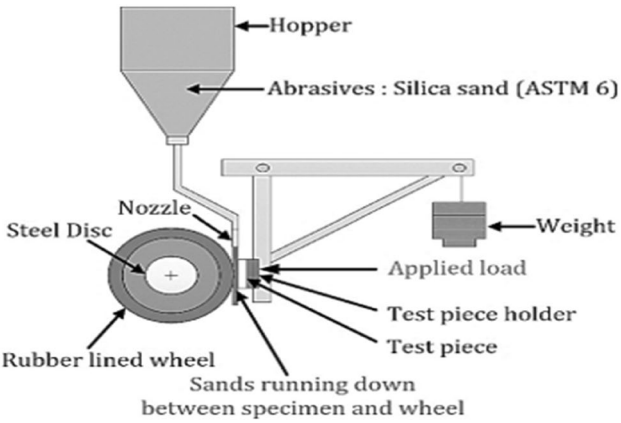

Fig. 6 Schematic diagram of rubber wheel abrasion wear tester

3 Results and Conversation

3.1 Hardness

Figure 8 depicts the results of variation of hardness on A356-hematite mixtures of specimens without and with copper chill at various weight percentages of reinforcement. The outcome demonstrates that the proportion of reinforcement increases with increase in hardness value. A356 alloy blend with 9% hematite has a higher hardness value than other compositions. It was also noted that the samples of copper chilled composite are tougher than composites of without copper chill because of existence of magnesium oxide and the iron oxide in the composites which also effects in upsurge of hardness in the material. The rapid cooling rate influences in enhancement of hardness value in composite material [14, 24, 25].

3.2 Tensile Strength

Figure 9 display the variation of tensile strength on wt% of hematite in the alloy A356 with and without copper chill specimen. Result shows that the tensile strength of the A356-hematite particulate composite rises with increase in weight percentage of reinforcement in the matrix alloy up to 9 wt%; further there was consequent reduction in tensile strength is due to lack of bonding amongst the reinforcement and matrix alloy. The 9 wt% of chilled specimens shows higher tensile strength than without copper chill specimens due to the strong bonding between the hard hematite Fe_2O_3 particles and the matrix alloy [9, 26–28].

3.3 Abrasive Wear

3.3.1 Consequence of Reinforcement

Figure 10 depicts the effect of abrasive wear loss (weight loss) on without and with copper chill A356 composites containing hematite particles. The three body abrasion wear findings of all specimens assessed shows that no hematite particles were plucked from the matrix alloy. This demonstrates the excellent interfacial adhesion amongst the hematite particles and the alloy matrix. It was also noted that the wear performance of particle reinforced mixtures primarily depend on the type of interfacial bond amongst the alloy matrix and the reinforcement. Further study showed that reduction in weight loss within upsurge in weight percentage of reinforcement specifies higher hardness of composites. Al A356 contains 7.25% of Silicon (Si) mixed with hematite (contains magnesium oxide) which is acts as adhesion properties. Thus, the formation of intermetallic precipitates of $MgSi0_2$ in the composite material after the chill casting process. The presence of intermetallic phases at greater

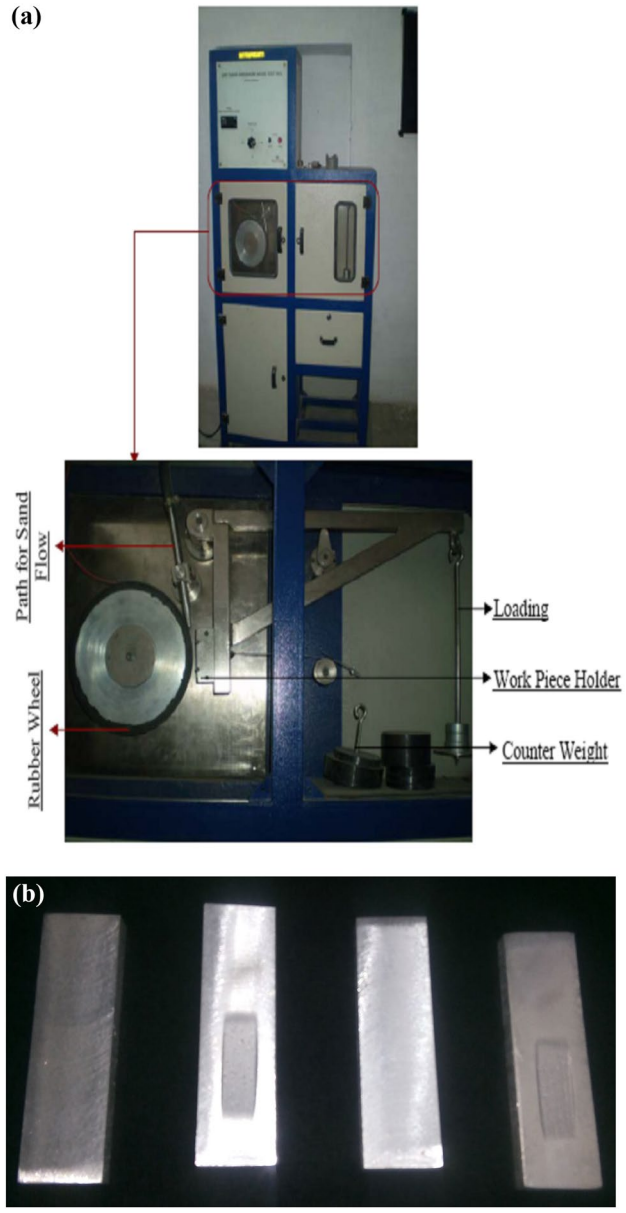

Fig. 7 **a** Dry sand abrasion test apparatus. **b** Specimens before and after wear test

extent which results in enhanced hardness and limits the penetration of particles on the surface of the A356 alloy and its composite. Copper chill specimens have better abrasion resistance of wear than without copper chill specimens and composites [11, 23, 29].

3.3.2 Consequence of Load

Figures 11 and 12, signifies the three body dry sand abrasive weight loss reported as wear loss for without and with copper chillA356-hematite particulate composite. Both the speed of 200 rpm and the duration of 30 min are held constant for all specimens with applied loads ranging from 2 to 10N in 2N steps. The outcome depicts that the reduction of abrasive wear rate with increase in the hematite particulates at diverse weight percentages into A356 matrix alloy. Further investigation revealed a considerable development in wear resistance in copper chill A356—hematite particle composites when compared to the composites of without copper chill. When the applied load was increased to a maximum of 10N, it was noted that there was a reduction in weight loss and no plucking amongst the reinforcement and the matrix [14]. The incorporation of particles of hematite into the ductile alloy of A356 matrix limits the penetration of abrasive particles onto the surface. An upsurge in abrasive resistance of wear leads to improvement in hardness. Hardness of the composites increased due to the presence of MgO and Fe_2O_3 which causes the prohibiting of A356 matrix grain growth during solidification and enhancement the density of the dislocations [30–32].

Table 5 Details of sand abrasive wear test apparatus

Sl. no.	Description	Particulars
1	Abrasive material	AFS 50–70 test sand
2	Rubber wheel speed	200 rpm through a helical geared motor of 1.5 kw (3 phase)
3	Test load	1 to 45
4	Rubber wheel diameter	228 mm
5	Power	430 V AC (3 Phase)
6	Specimen dimension	75 × 24 × 8 mm
7	Erodent	AFS3080
8	Sand mass flow rate	0.25 kg/min or 2.45 N/min
9	Rubber hardness	60–62 shore A
10	Duration	30 min
11	Pressure	5.88 N/mm^2
12	Load	12.75 N

3.4 Micrographic Analysis

According to the micrograph results, hematite particles appear to be discrete uniformly all over the A356 matrix at varied weight percentages, as exhibited in Fig. 13a to e. This can be attributed to effective stirring with appropriate process parameters. The homogeneous dispersion of hematite elements improves the tribological properties of the mixtures, and utilising copper chill, the rapid chilling rate forces a fine-grained structure, which improves the mechanical and tribological capabilities [14, 23].

The A356-9wt% of hematite composite elemental analysis is revealed in Fig. 14, which verifies the existence of elements including Al, Fe_2O_3, MgO, Cu, CaO, Si, and Zn. Through XRD examination, the presence of Fe_2O_3 and MgO

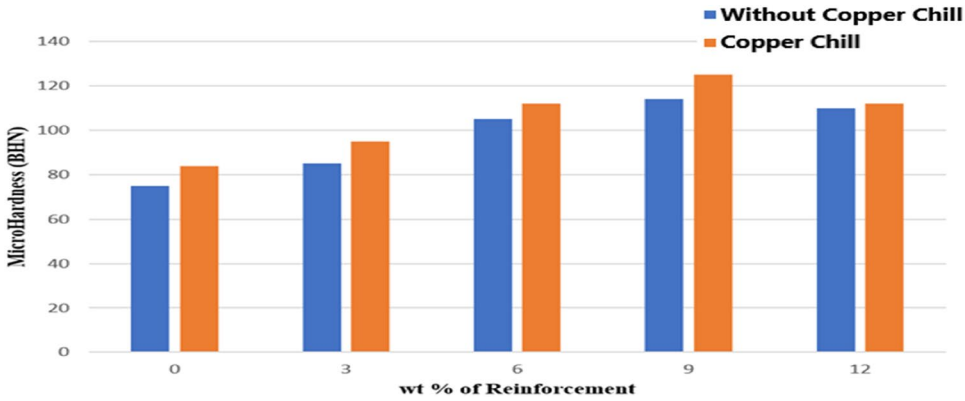

Fig. 8 Variation of hardness of composite on hematite wt% in A356 alloy, without and with copper chill

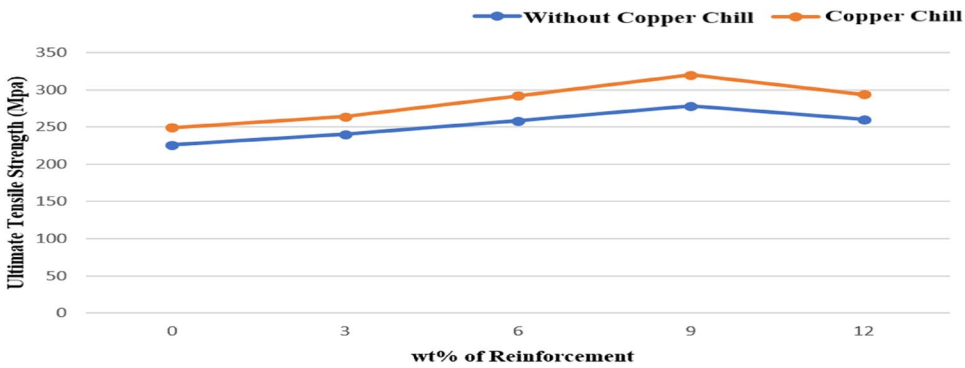

Fig. 9 Tensile strength variation on wt % of hematite in the alloy A356 in specimens with and without copper chill

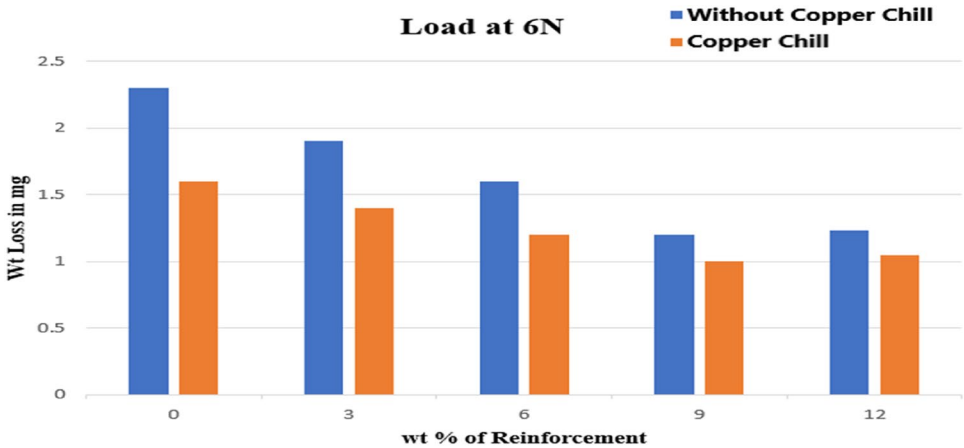

Fig. 10 Consequence of weight loss of A356 with hematite particulate composite for both without and with copper chill samplings

is used to confirm the dispersion of particles of hematite in the alloy of A356 composite. Figure 15a depicts alloy of A356 XRD pattern with varied aluminium phases are existing at numerous peaks. 39°, 45°, 65°, and 78° with numerous intensities. The peak intensity of the Al phase is 39°. The Fig. 15b displays the phases of Al and Fe_2O_3 in the XRD pattern of the A356 alloy with 9 weight percent of hematite particles. The produced composite JCPDS pattern is 98-6077 at various 2θ angles with varying intensities, and hematite phase can be found at angles of 29°, 47°, 56°, and 78°.

3.5 Fractography Studies

The Fig. 16 demonstrates the SEM photos of fractograph of A356/9 wt% of alloy and its composite for with and without copper chill. It was noticed from the SEM that, the clear inferences are often drawn with reference to the mode of fracture which is brittle, signified by the cleavage facets form the transgranular crystallographic plane &cleavage, is a characteristic of transgranular brittle fracture [23]. A Clear indication of intergranular fracture, identifiable by its "rock candy" presence, arises when the crack path follows grain

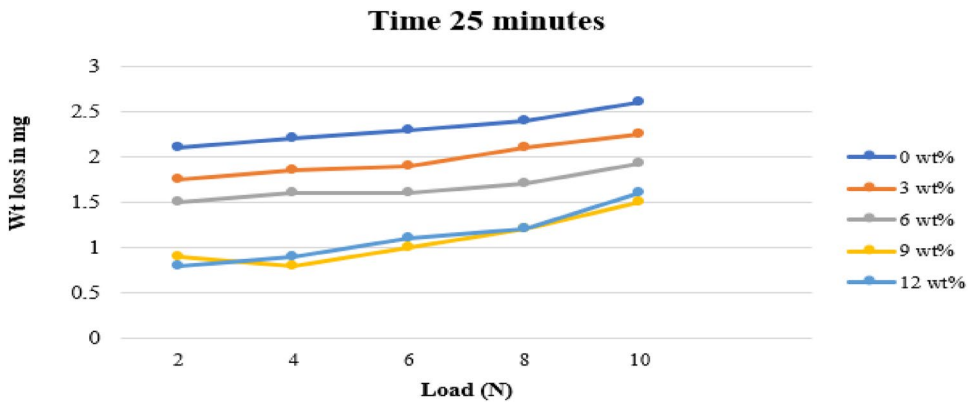

Fig. 11 Effect of changing hematite wt% in A356 on weight loss without copper chill

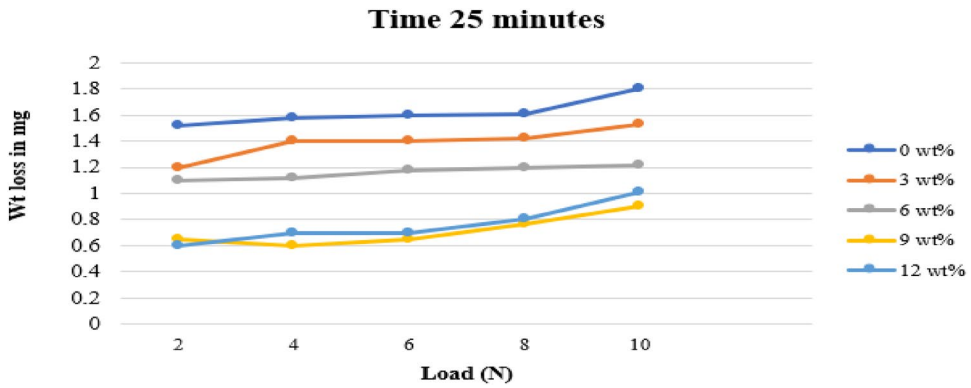

Fig. 12 Effect of changing hematite wt% in A356 on weight loss with copper chill

margins. The semi-elliptical lines are observed in the fractograph are a sign of striations. Each successive stress cycle marks the crack front position as it spreads outward from the origin. The arrangement of fatigue striations is naturally very uniform [12].

3.6 Worn Out Surface Morphology

Figure 17a–d shows the SEM pictures of abrasive wear worn surfaces of without and with copper chill alloy of A356 and its composites respectively. It was observed from the SEM that, an extensive plastic grooving and ploughing was noticed in the without copper chill A356 alloy compared to A356 alloy with copper chill, because of hardness and chilling effect. When related to matrix alloy, the extent of grooving in composites was limited. Further, the grooves were fine with minimal plastic deformation being noticed in the case of chilled composites. In case of matrix alloy, the abrasive particles were capable to dig-in and plough out the material owing to their lower hardness whereas in composite materials, the abrasive particles do scratch on the surfaces rather than ploughing out leading to lower material exclusion [14]. The abrasive wear resistance of the composites was significantly increased because of excellent interfacial bonding between hematite particles and matrix alloy. It was also pragmatic that amongst all the systems deliberate, copper chill used composites showed the less amount of grooving as exposed in Fig. 17d [32–34]. When compared to without copper chills, the surface of the wear out composite material for 9 wt% reinforcement with copper chill is exceptionally smooth. The results of the wear test experiments also support to this.

4 Conclusion

The sand casting procedure with and without copper chill was used to create the A356-hematite particle reinforced composites. The following observations below were made.

- The microstructural investigation clearly demonstrates that hematite particles are distributed uniformly in the A356 alloy matrix and its composites.
- Hematite particles and its phases are confirmed by the XRD analysis in the matrix of the A356 alloy.
- According to the experimental findings, the composite with 9 weight percent of hematite reinforced with A356 alloy demonstrates greater hardness and tensile strength than other compositions.
- It was also found that, due to the incidence of magnesium oxide and iron oxide in the composites, which influence an increase in hardness, as well as the chilling

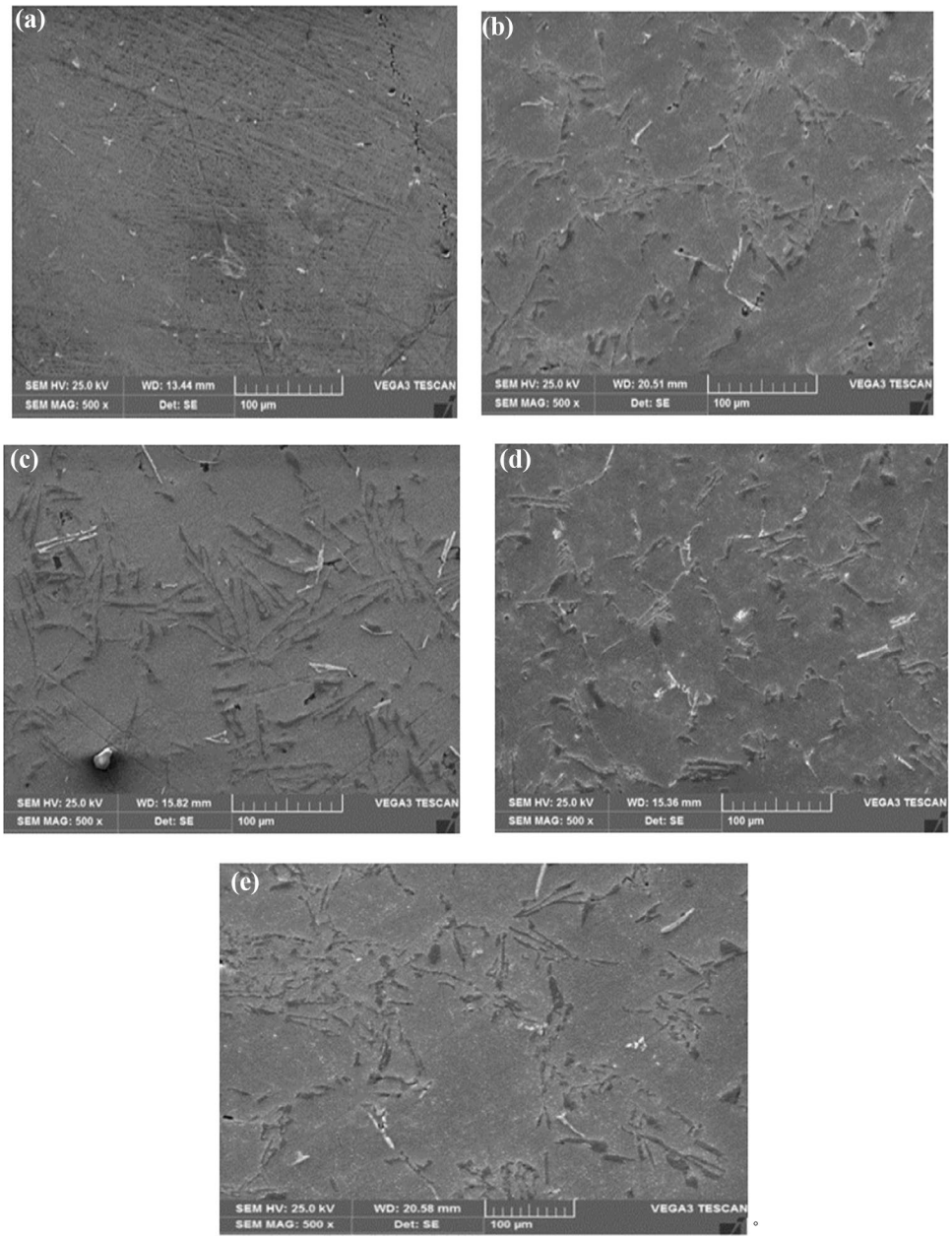

Fig. 13 SEM photos-graph at 500× magnification on **a** A356 Alloy, **b** A356-3 Wt% Composite, **c** A356-6wt% Composites, **d** A356-9wt% Composite, **e** A356-12 Wt% composite with copper chill

effect, which alters the rate of solidification, were also discovered to increase the hardness and toughness of the specimens of copper chilled composite in comparison to specimens without copper chill.

- The abrasive wear rate (wt loss in mg) reduces with increasing reinforcement wt%, further with an increase in applied load, the wear rate also rises. Additionally, the size and volume proportion of the reinforced particles affect wear rate.
- It was noticed that the composite with 9wt% hematite reinforced with alloy of A356 displays strong resistance of wear when related to compositions of other. It was also discovered that copper chilled composite specimens are tougher than specimens of without-copper chilled composites due to the occurrence of iron oxide and magnesium oxide in the composites, which also effects the increase of abrasive wear resistance by strengthen, toughness, and hardness.
- It was found that compared to without copper chills, the worn-out surface of the composite 9 wt% of reinforcement is very smooth. The specimens of copper chill acts as heat treatment has an advantageous consequence on abrasive resistance of wear of alloy matrix of A356 and it's composite. The enhanced wear resistance is demonstrated using SEM photos of worn surfaces.

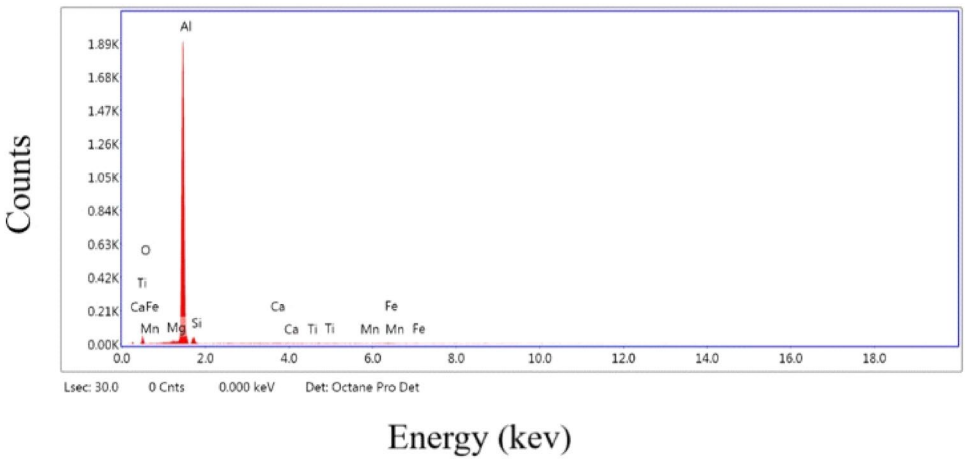

Fig. 14 A356 with 9wt% of particulates of hematite composite EDS spectrum shows the existence of particles of Fe_2O_3

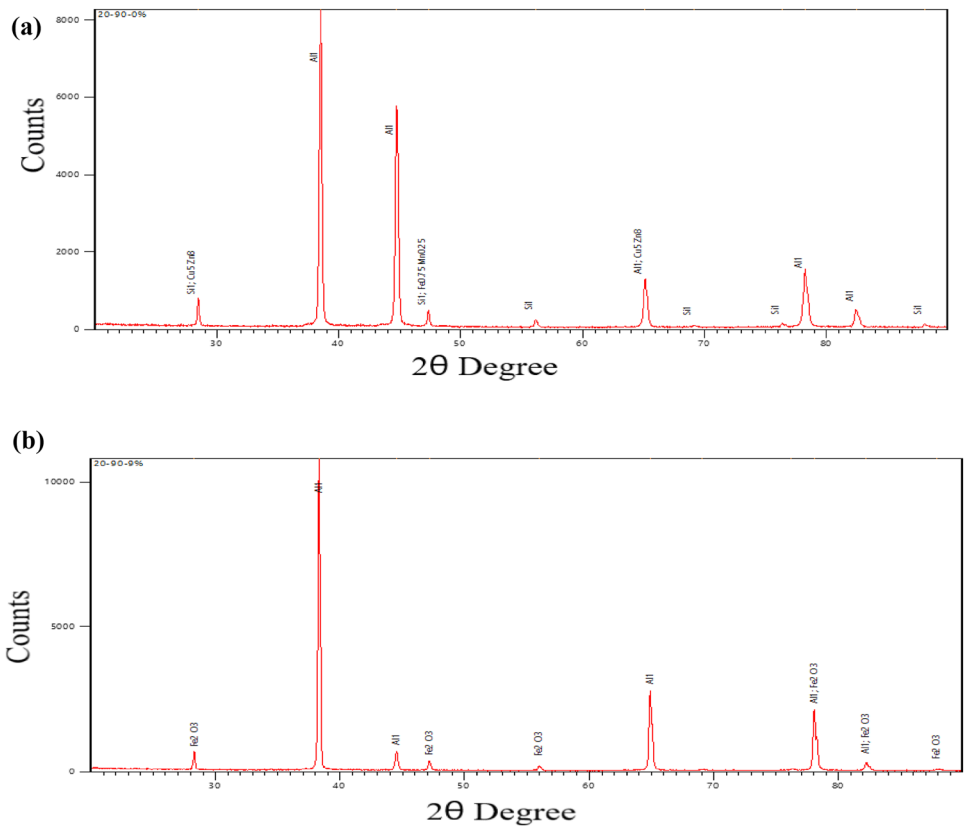

Fig. 15 **a** A 356 alloy X- Ray diffraction pattern. **b** 356-9wt% of hematite X-Ray diffraction pattern

- From the fractography study, It was clear that mode of fracture is a brittle in nature, signified by the cleavage facets form the transgranular crystallographic plane and striations.
- Based on the overall research outcomes, hematite has a significant impact in improving the mechanical and wear resistance of AMMCs.

Supplementary Information The online version contains supplementary material available at https://doi.org/10.1007/s40735-023-00755-8.

Acknowledgements The authors acknowledge Dr. Sathisha N, Professor & Head, Mechanical department YIT, Moodbidri. Dr. Jagannatha N. Professor and Head, Mechanical department, SJMIT, Chitradurga for their encouragement and support for manuscript revising.

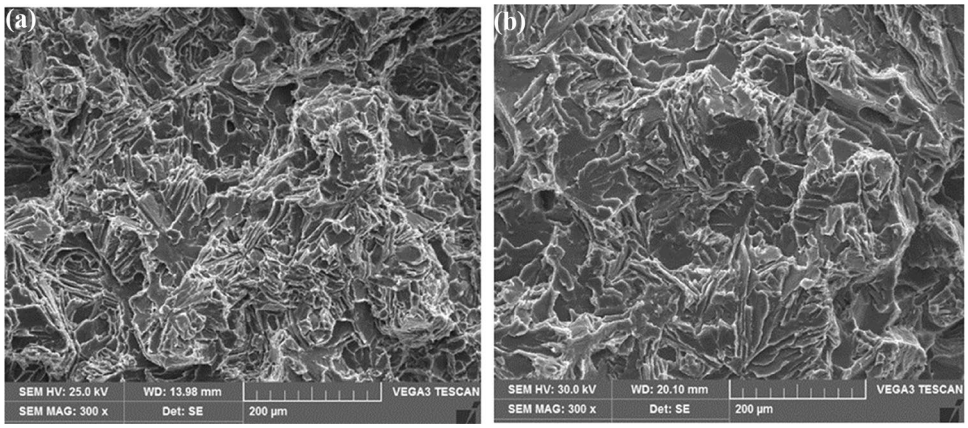

Fig. 16 Shows the Fractography of **a** A356/9wt% composite, **b** A356/9wt% composite with coper chill

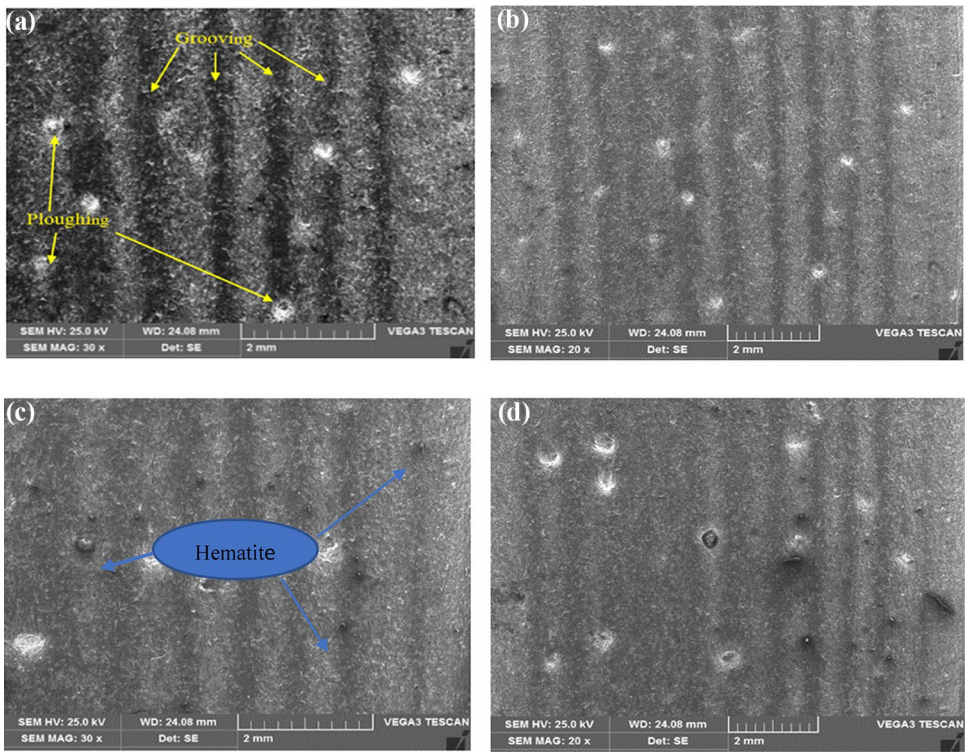

Fig. 17 SEM Photographs of abrasive wear worn surfaces of **a** A356 alloy, **b** A356 alloy with copper chill, **c** A356/9wt% composite, **d** A356/9wt% composite with coper chill

Authors Contributions Mr. MSK, Dr NS, Dr NJ are equally contributed to this work, for the preparation of the manuscript.

Funding The authors declare that no funds, grants, or other support were received during the preparation of this manuscript.

Data Availability Not Applicable.

Declarations

Competing interests The author have no relevant financial or non-financial interests to disclose.

Ethical Approval Not applicable.

Consent to Participate All Authors have agreed to participate in this research.

Consent for Publication Each of the named authors is aware of the content of the article and his given their consent for it to be published.

References

1. ASM Handbook Properties and Selection (1990) Nonferrous Alloys and Special-Purpose Materials 2:1–1328
2. ASM Handbook (1996) Fatigue and Fracture, vol 19, pp 1-2592

3. Heinz A, Haszler A, Keidel C, Moldenhauer S, Benedictus R, Miller WS (2000) Recent developments in aluminum alloys for aerospace applications. Mater Sci Eng 280(1):102–107. https://doi.org/10.1016/S0921-5093(99)00674-7Get
4. Seah KHW, Hemanth J, Sharma SC, Rao KVS (1999) Solidification behavior of water-cooled and sub-zero chilled cast iron. J Alloys Compds 290(1–2):172–180. https://doi.org/10.1016/S0925-8388(99)00224-8
5. Naeem HT, Abdullah FF (2019) Effects of garnet particles and chill casting conditions on properties of aluminum matrix hybrid composites. Eclética Química J 44(2):45–52. https://doi.org/10.26850/1678-4618eqj.v44.2.p45-52
6. Hiremath A, Hemanth J (2017) Experimental evaluation of the chill casting method for the fabrication of LM-25 aluminum alloy-borosilicate glass(p) composites. In: Advanced Materials and Engineering Materials VI ISSN:1662–9795, vol 748© Trans Tech Publications, Switzerland, pp 69–73. https://doi.org/10.4028/www.scientific.net/KEM.748.69
7. Gowda H, Prasad PR(2016) Evaluation of mechanical properties of A356 alloy based hybrid composite at different aging conditions. Int J Sci Res Publ 6(8)
8. Jamwal A, Vates UK, Gupta P, Aggarwal A, Sharma BP (2019) Fabrication and characterization of Al_2O_3–TiC-reinforced aluminum matrix composites. In: Advances in industrial and production engineering. Springer, Singapore, pp-349–356. https://doi.org/10.1007/978-981-13-6412-9_33
9. Kumar A, Arafath MY, Gupta P, Kumar D, Hussain CM, Jamwal A (2020) Microstructural and mechano-tribological behavior of Al reinforced SiC-TiC hybrid metal matrix composite. Mater Today 21(3):1417–1420
10. Opapaiboon J, Ayudhaya MS, Sricharoenchai P, Inthidech S, Matsubara Y (2018) Effect of chromium content on the three-body-type abrasive wear behavior of multi-alloyed white cast iron. J Met Mater Miner 28(2):94–105
11. Rakshath S, Suresha B, Sasi Kumar R, Saravanan I (2019) Dry sliding and abrasive wear behaviour of Al-7075 reinforced with alumina and boron nitride particulates. Mater Today Proc 22(1):619–626. https://doi.org/10.1016/j.matpr.2019.09.010
12. Bandekar N, Prasad MA (2017) Fractographic and three body abrasion behaviour of Al-Garnet-C hybrid chill cast composites. IOP Conf Ser 225:1–6. https://doi.org/10.1088/1757-899X/225/1/012290
13. VijayKumarVikranthKannanthVinay SLMSDR (2015) Three body abrasive wear study on A356 aluminum alloy under T6 heat treated conditions. AmJ Mater Sci 5:43–47. https://doi.org/10.5923/c.materials.201502.09
14. Nagaral M, Auradi V, Kori SA, Hiremath V (2019) Investigation on mechanical and wear behavior of nano Al_2O_3 particulates reinforced AA7475 alloy composites. J Mech Eng Sci 13:4623–4635. https://doi.org/10.15282/jmes.13.1.2019.19.0389
15. Sunil Kumar M, Sathisha N, Jagannatha N, Chandra BT (2022) Tribological study on effect of chill casting on aluminium A356 reinforced with hematite paticulated composites. J Bio Tribo Corros 8:52. https://doi.org/10.1007/s40735-022-00635-7
16. Garg P, Jamwal A, Kumar D, Sadasivuni KK, Hussain CM, Gupta P (2019) Advance research progresses in aluminium matrix composites: manufacturing & applications. J Mater Res Technol 8(5):4924–4939. https://doi.org/10.1016/j.jmrt.2019.06.028
17. Radhika N (2018) Analysis of three body abrasive wear behaviour of centrifugally cast aluminium composite reinforced with Ni coated SiC using Taguchi technique. Tribol Ind 40(1):81–91. https://doi.org/10.24874/ti.2018.40.01.07
18. Sunil Kumar M, Sathisha N, Chandra BT (2021) A study on effect of chill casting on A356 reinforced with hematite metal matrix composite. Mater Today Proc 35(Part3):450–455. https://doi.org/10.1016/j.matpr.2020.02.963
19. Gupta P, Kumar D, Parkash OM, Jha AK (2013) Structural and mechanical behavior of 5% Al_2O_3 reinforced Fe metal matrix composites (MMC) produced by powder metallurgy (P/M) route. Bull Mater Sci 36(5):859–868. https://doi.org/10.1007/s12034-013-0545-1
20. Jha P, Gupta P, Kumar D, Parkash O (2014) Synthesis and characterization of Fe-ZrO_2 metal matrix composites. J Compos Mater 48(17):2107–2115
21. Garg P, Gupta P, Kumar D, Parkash O (2016) Structural and mechanical properties of graphene reinforced aluminum matrix composites. J Mater Environ Sci 7(5):1461–1473
22. Kok M (2011) Computational investigation of testing parameter effects on abrasive wear behaviour of Al_2O_3particle-reinforced MMCs using statistical analysis. Int J Adv Manuf Technol 52(1–4):207–215. https://doi.org/10.1007/s00170-010-2734-z
23. Sharma P, Khanduja D, Sharma S (2016) Dry sliding wear investigation of Al6082/Gr metal matrix composites by response surface methodology. J Market Res 5:29–36. https://doi.org/10.1016/j.jmrt.2015.05.001
24. Ahamad N, Mohammad A, Sadasivuni KK, Gupta P (2020) Structural and mechanical characterization of stir cast Al–Al_2O_3–TiO_2 hybrid metal matrix composites. J Compos Mater 54(21):2985–2997. https://doi.org/10.1177/0021998320906207
25. Ahamad N, Mohammad A, Sadasivuni KK, Gupta P (2020) Phase, microstructure and tensile strength of Al–Al_2O_3–C hybrid metal matrix composites. Proc Inst Mech Eng Part C 234(13):2681–2693. https://doi.org/10.1177/0954406220909846
26. Jamwal A, Mittal P, Agrawal R, Gupta S, Kumar D, Sadasivuni KK, Gupta P (2020) Towards sustainable copper matrix composites: manufacturing routes with structural, mechanical, electrical and corrosion behaviour. J Compos Mater 54(19):2635–2649. https://doi.org/10.1177/0021998319900655
27. Hossain S, Rahman MM, Chawla D, Kumar A, Seth PP, Gupta P, Kumar D, Agrawal R, Jamwal A (2020) Fabrication, microstructural and mechanical behavior of Al-Al_2O_3-SiC hybrid metal matrix composites. Mater Today 21(Part 3):1458–1461. https://doi.org/10.1016/j.matpr.2019.10.089
28. Bandil K, Vashisth H, Kumar S, Verma L, Jamwal A, Kumar D, Singh N, Sadasivuni KK, Gupta P (2019) Microstructural, mechanical and corrosion behaviour of Al–Si alloy reinforced with SiC metal matrix composite. J Compos Mater 53(28):4215–4223. https://doi.org/10.1177/0021998319856679
29. Gupta P, Kumar D, Parkash OM, Jha AK (2014) Effect of sintering on wear characteristics of Fe-Al_2O_3 metal matrix composites. Proc Inst Mech Eng Part J 228(3):362–368. https://doi.org/10.1177/1350650113508934
30. Ahamad N, Mohammad A, Sadasivuni KK, Gupta P (2021) Wear, optimization and surface analysis of Al-Al_2O_3-TiO_2 hybrid metal matrix composites. Proc Inst Mech Eng Part J 235(1):93–102. https://doi.org/10.1177/1350650120970432
31. Jamwal A, Seth PP, Kumar D, Agrawal R, Sadasivuni KK, Gupta P (2020) Microstructural, tribological and compression behaviour of Copper matrix reinforced with Graphite-SiC hybrid composites. Mater Chem Phys 251:123090. https://doi.org/10.1016/j.matchemphys.2020.123090
32. Sohag MA, Gupta P, Kondal N, Kumar D, Singh N, Jamwal A (2020) Effect of ceramic reinforcement on the microstructural, mechanical and tribological behavior of Al-Cu alloy metal matrix composite. Mater Today 21(Part 3):1407–1411. https://doi.org/10.1016/j.matpr.2019.08.179
33. Radhika N, Sai Charan K (2017) Experimental analysis on three body abrasive wear behaviour of stir cast Al LM 25/TiC metal matrix composite. Trans Indian Inst Met 70(9):2233–2240. https://doi.org/10.1007/s12666-017-1061-6
34. Agarwal G, Patnaik A, Sharma RK (2014) Comparative investigations on three-body abrasive wear behavior of long and short

glass fiber reinforced epoxy composites. Adv Compos Mater 23:293–317. https://doi.org/10.1080/09243046.2013.868661